Mech. Struct. & Mach., TBIP(TBIP), 1–24 (TBIP)

Solving Nonconvex Problems of Multibody Dynamics with Joints, Contact and Small Friction by Successive Convex Relaxation

Mihai Anitescu * and Gary D. Hart[1]

Department of Mathematics, University of Pittsburgh, Pittsburgh, PA 15260, U.S.A.

Time-stepping methods using impulse-velocity approaches are guaranteed to have a solution for any friction coefficient, but they may have nonconvex solution sets. We present an example of a configuration with a nonconvex solution set for any nonzero value of the friction coefficient. We construct an iterative algorithm that solves convex subproblems and that is guaranteed, for sufficiently small friction coefficients, to retrieve, at a linear convergence rate, the velocity solution of the nonconvex linear complementarity problem whenever the frictionless configuration can be disassembled. In addition, we show that one step of the iterative algorithm provides an excellent approximation to the velocity solution of the original, possibly nonconvex, problem if the product between the friction coefficient and the slip velocity is small.

*The work of this author was supported by the National Science Foundation, through the award DMS-9973071, as well as the Mathematical, Information, and Computational Sciences Division subprogram of the Office of Advanced Scientific Computing, U.S. Department of Energy, under Contract W-31-109-Eng-38

[1]The work of this author was supported by the Central Research and Development Fund of the University of Pittsburgh

1. Introduction

Multi-rigid-body dynamics with joints, contact and friction is fundamental for virtual reality and robotics simulations. However, the Coulomb model for friction poses several obstacles in the path of efficient simulation. The classical acceleration-force approach does not necessarily have a solution even in the simple case of a rod in contact with a table top at high friction [22, 23]. Recently, time-stepping methods have been developed in an impulse-velocity framework that avoid the inconsistencies that may appear in the classical approach [3, 4, 23, 22]. The methods are related to the complementarity-based collision resolution methods in [12, 13], but they are extended to apply to non-colliding states of multi-body systems with joints, contact and friction. These methods can be modified to accommodate the most common types of stiffness [2]. When there is no friction, these time-stepping algorithms solve, at every step, a linear complementarity problem that represents the optimality conditions for a convex quadratic program.

When the friction coefficients are nonzero, however, this interpretation is lost and the solution set may be nonconvex, even for small friction coefficients as we show with an example, which may increase the computational effort of finding a solution. In this work we attempt to find a solution to the possibly nonconvex linear complementarity problem by using an algorithm that solves convex subproblems and has an upper bounded linear convergence rate, at least for small friction coefficients.

2. The Linear Complementarity Subproblem of the Time-Stepping Scheme

In the following q and v constitute, respectively, the generalized position and, respectively, generalized velocity vector of a system of several bodies [15].

A. Model Constraints

In describing the model, we follow the framework and notations from [2, 3, 4, 22].

Our approach covers several types of constraints. In the following we say that the variables a, b are complementary if $a \geq 0$, $b \geq 0$ and $ab = 0$, which we denote by $a \geq 0 \perp b \geq 0$. For vectors, such a relationship is to be understood componentwise.

Joint Constraints. Such constraints are described by the equations

$$\Phi_j^{(i)}(q) = 0,\ i = 1, 2, \ldots, m\,. \tag{1}$$

Here, $\Phi_j^{(i)}(q)$ are sufficiently smooth functions. We denote by $\nu^{(i)}(q)$ the gradient of the corresponding function, or

$$\nu^{(i)}(q) = \nabla_q \Phi_j^{(i)}(q), \quad i = 1, 2, \ldots, m.$$

The impulse exerted by a joint on the system is $c_\nu^{(i)} \nu^{(i)}(q)$, where $c_\nu^{(i)}$ is a scalar related to the Lagrange multiplier of classical constrained dynamics [15].

Noninterpenetration Constraints. These constraints are defined in terms of a continuous signed distance function between the two bodies $\Phi_c(q)$ [6]. The noninterpenetration constraints become

$$\Phi_c^{(j)}(q) \geq 0, \quad j = 1, 2, \ldots, p. \tag{2}$$

The function $\Phi_c(q)$ is generally not differentiable, especially when the bodies have flat surfaces. Usually, this situation is remediable by considering different geometric primitives [10] that result in noninterpenetration constraints being expressed in terms of several inequalities involving differentiable functions $\Phi_c(q)$. In the following, we may refer to (j) as the *contact (j)*, though the contact is truly active only when $\Phi_c^{(j)}(q) = 0$. We denote the normal at contact (j) by

$$n^{(j)}(q) = \nabla_q \Phi_c^{(j)}(q),\ j = 1, 2, \ldots, p. \tag{3}$$

When the contact is active, it can exert a compressive normal impulse, $c_n^{(j)} n^{(j)}(q)$ on the system, which is quantified by requiring $c_n^{(j)} \geq 0$. The fact that the contact must be active before a nonzero compression

impulse can act is expressed by the complementarity constraint

$$\Phi_c^{(j)}(q) \geq 0 \perp c_n^{(j)} \geq 0,\ j = 1, 2, \ldots, p.$$

Frictional Constraints. These are expressed by means of a discretization of the friction cone [2, 3, 22]. For a contact j, we take a collection of coplanar vectors $d_i(q)$, $i = 1, 2, \ldots, m_C$, which span the plane tangent at the contact (though the plane may cease to be tangent to the contact normal when mapped in generalized coordinates [6]). The cover of the vectors $d_i(q)$ should approximate the transversal shape of the friction cone. In two-dimensional mechanics, the tangent plane is one dimensional, its transversal shape is a segment, and only two such vectors $d_1(q)$ and $d_2(q)$ are needed in this formulation. We denote by $D(q)$ a matrix whose columns are $d_i(q)$, $i = 1, 2, \ldots, m_C$, or $D(q) = [d_1(q), d_2(q), \ldots, d_{m_C}(q)]$. A tangential impulse is $\sum_{i=1}^{m_C} \beta_i d_i(q)$, where $\beta_i \geq 0$, $i = 1, 2, \ldots, m_C$. We assume that the tangential contact description is symmetric, that is, that for any i there exists a j such that $d_i(q) = -d_j(q)$.

The friction model ensures maximum dissipation for given normal impulse c_n and velocity v and guarantees that the total contact impulse is inside the discretized cone. We express this model as

$$\begin{aligned} D(q)^T v + \lambda e \geq 0 \perp \beta \geq 0, \\ \mu c_n - e^T \beta \geq 0 \perp \lambda \geq 0. \end{aligned} \tag{4}$$

Here e is a vector of ones of dimension m_C, $e = (1, 1, \ldots, 1)^T$, μ is the friction parameter, and β is the vector of tangential impulses $\beta = (\beta_1, \beta_2, \ldots, \beta_{m_C})$. The additional variable λ is approximately equal to the norm of the tangential velocity at the contact, if there is relative motion at the contact, or $\|D(q)^T v\| \neq 0$ [3, 22].

Notations. We denote by $M(q)$ the symmetric, positive definite, mass matrix of the system in the generalized coordinates q and by $k(t, q, v)$ the external force. All quantities described in this section associated with contact j are denoted by the superscript $^{(j)}$. When we use a vector or matrix norm whose index is not specified, it is the 2 norm.

B. The Linear Complementarity Problem

To include these results in a time-stepping scheme, we formulate all geometrical constraints at the velocity level by linearization. To this end we assume that at the current time step we have exact feasibility of the noninterpenetration and joint constraints. This assumption can be practically satisfied if at the end of each integration step we do a projection onto the feasible manifold [2].

Let h_l be the time step at time $t^{(l)}$. If, at time $t^{(l)}$, the system is at position $q^{(l)}$ and velocity $v^{(l)}$, then we choose the new position to be $q^{(l+1)} = q^{(l)} + h_l v^{(l+1)}$, where $v^{(l+1)}$ is determined by enforcing the simulation constraints. For joint constraints the linearization leads to $\nabla_q \Phi_j^{(i)^T}(q^{(l)})v^{(l+1)} = \nu^{(i)^T}(q^{(l)})v^{(l+1)} = 0$. For one such noninterpenetration constraint j, $\Phi_c^{(j)}(q) \geq 0$, linearization at $q^{(l)}$ for one time step amounts to $\Phi_c^{(j)}(q^{(l)}) + h_l \nabla \Phi_c^{(j)^T}(q^{(l)})v^{(l+1)} \geq 0$, or

$$\nabla \Phi_c^{(j)^T}(q^{(l)})v^{(l+1)} + \frac{\Phi_c^{(j)}(q^{(l)})}{h_l} \geq 0. \tag{5}$$

Since we assume that at step (l) all geometrical constraints are satisfied, this implies that $\frac{\Phi_c^{(j)}(q^{(l)})}{h_l} \geq 0$. For computational efficiency, only the contacts that are imminently active are included in the dynamical resolution and linearized, and their set is denoted by $\mathcal{A}$. One practical way of determining $\mathcal{A}$ is by including all j for which $\Phi_c^{(j)}(q) \leq \delta$, where δ is a sufficiently small quantity, perhaps dependent on the size of the velocity. After $v^{(l+1)}$ is determined, one can decide that the contact (j) is active if $c_n^{(j)}$, the variable that is complementary to the inequality (5), is positive.

If a contact switches from inactive to active, a collision resolution, possibly with energy restitution, needs to be applied [3]. In this work we assume that no energy lost during collision is restituted; hence we avoid the need to consider a compression followed by decompression linear complementarity problem.

After collecting all the constraints introduced above, with the geometrical constraints replaced by their linearized versions, we obtain

the following mixed linear complementarity problem.

$$\begin{bmatrix} M^{(l)} & -\widetilde{\nu} & -\widetilde{n} & -\widetilde{D} & 0 \\ \widetilde{\nu}^T & 0 & 0 & 0 & 0 \\ \widetilde{n}^T & 0 & 0 & 0 & 0 \\ \widetilde{D}^T & 0 & 0 & 0 & \widetilde{E} \\ 0 & 0 & \widetilde{\mu} & -\widetilde{E}^T & 0 \end{bmatrix} \begin{bmatrix} v^{(l+1)} \\ c_\nu \\ c_n \\ \widetilde{\beta} \\ \lambda \end{bmatrix} + \begin{bmatrix} -Mv^{(l)} - h_l k^{(l)} \\ 0 \\ \Delta \\ 0 \\ 0 \end{bmatrix} = \begin{bmatrix} 0 \\ 0 \\ \rho \\ \widetilde{\sigma} \\ \zeta \end{bmatrix} \tag{6}$$

$$\begin{bmatrix} c_n \\ \widetilde{\beta} \\ \lambda \end{bmatrix}^T \begin{bmatrix} \rho \\ \widetilde{\sigma} \\ \zeta \end{bmatrix} = 0, \qquad \begin{bmatrix} c_n \\ \widetilde{\beta} \\ \lambda \end{bmatrix} \geq 0, \qquad \begin{bmatrix} \rho \\ \widetilde{\sigma} \\ \zeta \end{bmatrix} \geq 0\,. \tag{7}$$

Here $\widetilde{\nu} = [\nu^{(1)}, \nu^{(2)}, \ldots, \nu^{(m)}]$, $c_\nu = [c_\nu^{(1)}, c_\nu^{(2)}, \ldots, c_\nu^{(m)}]^T$, $\widetilde{n} = [n^{(j_1)}, n^{(j_1)}, \ldots, n^{(j_s)}]$, $c_n = [c_n^{(j_1)}, c_n^{(j_2)}, \ldots, c_n^{(j_s)}]^T$, $\widetilde{\beta} = [\beta^{(j_1)T}, \beta^{(j_2)T}, \ldots, \beta^{(j_s)T}]$, $\widetilde{D} = [D^{(j_1)}, D^{(j_2)}, \ldots, D^{(j_s)}]$, $\lambda = [\lambda^{(j_1)}, \lambda^{(j_2)}, \ldots, \lambda^{(j_s)}]$, $\widetilde{\mu} = diag(\mu^{(j_1)}, \mu^{(j_2)}, \ldots, \mu^{(j_s)})^T$, $\Delta = \frac{1}{h_l}\left(\Phi_c^{(j_1)}, \Phi_c^{(j_2)}, \ldots, \Phi_c^{(j_s)}\right)^T$ and

$$\widetilde{E} = \begin{bmatrix} e^{(j_1)} & 0 & 0 \cdots & 0 \\ 0 & e^{(j_2)} & 0 \cdots & 0 \\ \vdots & \vdots & \vdots \; \vdots & \vdots \\ 0 & 0 & 0 \cdots & e^{(j_s)} \end{bmatrix}$$

are the lumped LCP data, and $\mathcal{A} = \{j_1, j_2, \ldots, j_s\}$ are the active contact constraints. The vector inequalities in (7) are to be understood componentwise. We use the ˜ notation to indicate that the quantity is obtained by properly adjoining blocks that are relevant to the aggregate joint or contact constraints.

To simplify the presentation we do not explicitly include the dependence of the geometrical parameters on the data of the simulation. Also $M^{(l)} = M(q^{(l)})$ is the mass matrix, which we assume to be positive definite, at time (l), and $k^{(l)} = k(t^{(l)}, q^{(l)}, v^{(l)})$ represents the external force at time (l). Note that, since $\Delta \geq 0$, the results from [3] can be applied to show that the above linear complementarity problem is guaranteed to have a solution.

The way the model is described in (6–7) it can describe bodies in

contact and bodies that enter totally plastic collisions, even without doing explicit collision detection. Totally plastic collisions are essentially only a change of the active set and there is no need to modify (6–7) to accommodate them. Partially elastic collisions can be included if we combine our algorithm with a collision detection scheme [3, 22, 23] and we perform a compression-decompression approach with $h_l = 0$ and $\Delta = 0$. For the linear complementarity problems that appear in that case the following results continue to hold.

To establish our convergence results, we need several regularity assumptions concerning the problem (6–7), which we describe in this section.

The set of feasible constraint reaction impulses form the friction cone, that is

$$FC(q) = \left\{ t = \tilde{\nu} c_\nu + \tilde{n} c_n + \tilde{D}\tilde{\beta} \,\middle|\, c_n \geq 0,\ \tilde{\beta} \geq 0, \right. \\ \left. \|\beta^{(j)}\|_1 \leq \mu^{(j)} c_n^{(j)},\ \forall j \in \mathcal{A} \right\}. \tag{8}$$

We use the friction cone name for $FC(q)$ since for the case where there are no joint constraint, we recover the usual definition of a friction cone. The key notion is the one of a pointed friction cone.

Definition: We say that the friction cone $FC(q)$ is pointed if it does not contain any proper linear subspace.

By using duality, we obtain the following description of pointed friction cones:

$$\text{FC(q) is pointed} \iff \\ \left. \begin{array}{c} \left(c_\nu, c_n \geq 0, \tilde{\beta} \geq 0\right) \neq 0 \\ \|\beta^{(j)}\|_1 \leq \mu^{(j)} c_n^{(j)}, \forall j \in \mathcal{A} \end{array} \right\} \Longrightarrow \tilde{\nu} c_\nu + \tilde{n} c_n + \tilde{D}\tilde{\beta} \neq 0. \tag{9}$$

The last equation makes clear the physical interpretation of a pointed friction cone: There is no nonzero reaction impulse (or force) that results in a zero net action, i.e. the system or parts of it cannot get "jammed". Of interest to us will be the pointed friction cone notion when $\tilde{\mu} = 0$. In that case (9) becomes

$$\tilde{n} c_n + \tilde{\nu} c_\nu = 0,\ c_n \geq 0 \Rightarrow c_n = 0,\ c_\nu = 0.$$

It can be shown, again by using duality, that the above relation is

equivalent to the joint constraint matrix $\tilde{\nu}$ having linearly independent columns and

$$\exists v \text{ such that } \tilde{\nu}^T v = 0 \text{ and } \tilde{n}^T v > 0.$$

The latest condition means that the rigid body configuration can be disassembled [7]: there exists an external force that breaks all contacts while keeping feasibility of the joint constraints. This condition can be estimated visually for most simple configurations.

When a nonlinear program whose constraints are (1) and (2) satisfies the above relation, it is said to satisfy the Mangasarian Fromovitz constraint qualification or MFCQ [16, 17]. This property is essential to ensure the good behavior (Lipschitz continuity) of the solution of the nonlinear program with respect to its parameters [21]. Lipschitz continuity is the key element that allows us to show convergence of our fixed-point iteration (successive convex relaxation).

3. An Example of Configuration with Nonconvex Solution Set

If the friction coefficients are $\mu^{(j)} = 0$, $j \in \mathcal{A}$, then the mixed linear complementarity problem (6–7) has a positive semidefinite matrix and can be shown to always have a convex solution set. Such mixed linear complementarity problems can be solved by certain algorithms in a time that is polynomial with respect to the problem size [5], and the algorithms are called *polynomial* algorithms. This property is important, because pivotal methods, such as simplex for linear programming, are known to potentially need a number of pivots that grow exponentially with the size of the problem. Such effects are unlikely to appear for small-sized problems, but they may create an inconvenience for large-scale problems.

An important question is whether it can be guaranteed that the mixed linear complementarity problem (6–7) can be solved efficiently, preferably in polynomial time, at least for small friction coefficients.

Consider the configuration in Figure 1, where a body of mass m, shaped like a hexagonal pyramid, is in contact with a fixed tabletop

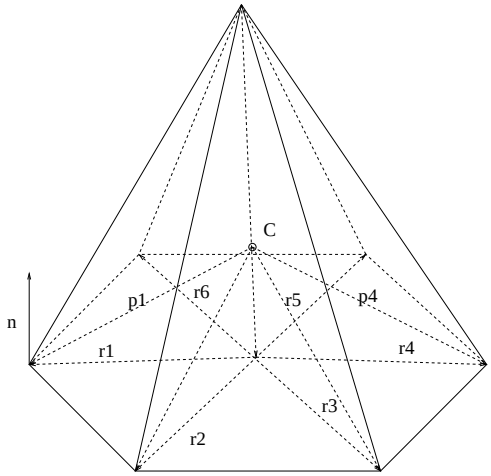

Figure 1. Example with a nonconvex solution set

(whose edges are not shown) in the position shown, for which we are going to set up the linear complementarity problem (6–7). In the following description we represent all relevant vectors with respect to the global three-dimensional space. The generalized coordinates [15] consist of the three translational coordinates and three rotational coordinates of the body about its center of mass C. In this section, we analyze only one step of the algorithm (6–7) and we denote the time-step h_l simply by h.

The contact configuration is represented by six point-on-plane contact constraints [6], one for each corner of the pyramid in contact with the tabletop. The normal at each contact in global coordinates is $\vec{n} = (0, 0, 1)^T$. From the center of mass C we have six vectors, $\vec{p}^{(j)}$, $j = 1, 2, \ldots, 6$, pointing toward the six bottom vertices of the pyramid and whose projection on the contact plane between the pyramid and the tabletop are $\vec{r}^{(j)}$, $j = 1, 2, \ldots, 6$. Note that $\vec{p}^{(j)} \times \vec{n} = \vec{r}^{(j)} \times \vec{n}$, for $j = 1, 2, \ldots, 6$, where $\times$ denotes the vector product. We assume that the bottom of the pyramid is a regular hexagon, which means that

we have

$$\vec{r}^{(1)} + \vec{r}^{(3)} + \vec{r}^{(5)} = 0, \quad \vec{r}^{(2)} + \vec{r}^{(4)} + \vec{r}^{(6)} = 0. \tag{10}$$

Since we will look only for solutions that have zero tangential impulse, we do not describe the tangential vectors. It can be immediately seen that the generalized normal becomes $n^{(j)} = \left(\vec{n}^T, \left(\vec{r}^{(j)} \times \vec{n}\right)^T\right)^T$, $j = 1, 2, \ldots, 6$. From the expression of the generalized normals and (10) we obtain

$$n^{(1)} + n^{(3)} + n^{(5)} = 3\begin{pmatrix}\vec{n}\\0\end{pmatrix}, \quad n^{(2)} + n^{(4)} + n^{(6)} = 3\begin{pmatrix}\vec{n}\\0\end{pmatrix}. \tag{11}$$

The mass matrix in the six coordinates is

$$M = \left(\begin{array}{c|c} m\mathbf{I}_{3\times 3} & \mathbf{0}_{3\times 3} \\ \hline \mathbf{0}_{3\times 3} & J \end{array}\right),$$

where J is the inertia matrix, which we assume to be symmetric positive definite.

We assume that the initial velocity of this configuration, $v^{(0)}$, is 0. The effect of the gravity is quantified by the external force vector

$$k = -g\begin{pmatrix}\vec{n}\\\mathbf{0}_3\end{pmatrix}.$$

We expect that the solution of (6–7) is $v^{(1)} = 0$. After we use all the above defined quantities in (6–7) we obtain the mixed linear complementarity problems

$$\begin{aligned} \textstyle\sum_{j=1}^{6} c_n^{(j)} n^{(j)} - hmg\begin{pmatrix}\vec{n}\\0\end{pmatrix} &= 0. \\ \mu c_n^{(j)} \geq 0 \perp \lambda^{(j)} \geq 0, \quad j &= 1, 2, \ldots, 6. \end{aligned}$$

Using (11), we have the following choices that satisfy these constraints, and, thus, constitute a part of the solution: of (6–7)

1. $c_n^{(1)} = c_n^{(3)} = c_n^{(5)} = \frac{hmg}{3}$, $c_n^{(2)} = c_n^{(4)} = c_n^{(6)} = 0$, $\lambda^{(1)} = \lambda^{(3)} = \lambda^{(5)} = 0$, $\lambda^{(2)} = \lambda^{(4)} = \lambda^{(6)} = 1$,
2. $c_n^{(1)} = c_n^{(3)} = c_n^{(5)} = 0$, $c_n^{(2)} = c_n^{(4)} = c_n^{(6)} = \frac{hmg}{3}$, $\lambda^{(1)} = \lambda^{(3)} = \lambda^{(5)} = 1$, $\lambda^{(2)} = \lambda^{(4)} = \lambda^{(6)} = 0$.

If, however, we take the average of the solutions, we obtain that $c_n^{(j)} = \frac{hmg}{6}$, $\lambda^{(j)} = \frac{1}{2}$, $j = 1, 2, \ldots, 6$ which violate the complementarity constraint

$$\mu c_n^{(j)} \geq 0 \ \perp \ \lambda^{(j)} \geq 0, \quad j = 1, 2, \ldots, 6,$$

as soon as $\mu > 0$ (the rest of the constraints must be satisfied because they are linear). This implies that the solution set of (6–7) is not convex for any nonzero friction coefficient.

Noconvexity of the solution set is significant mostly from the computational perspective. The largest class of linear complementarity problems like (6–7) for which existence of a polynomial (assymptotically fast) algorithm has been proven must have a convex solution set [5]. On the other hand the class of linear complementarity problems that have nonconvex solution sets contains reformulated instances of the knapsack problem which is known to be NP (non-polynomially or exponentially) hard. Therefore nonconvexity of the solution set of the linear complementarity problem significantly increases the likelihood that the problem is difficult.

4. Sequential Convex Relaxation of (6–7)

To address the nonconvexity issue, we develop in this section an iterative method that has a guaranteed rate of convergence to the velocity solution of (6–7) for sufficiently small but nonzero friction coefficients. The methods have convex subproblems that can be solved in polynomial time.

To simplify notation, we replace the superscript $(l + 1)$ of the velocity solution of (6–7) by $*$, and we use no superscript when defining the complementarity problems.

We first approximate the mixed linear complementarity problem

(6–7) by the following mixed linear complementarity problem:

$$\begin{bmatrix} M^{(l)} & -\widetilde{\nu} & -\widetilde{n} & -\widetilde{D} & 0 \\ \widetilde{\nu}^T & 0 & 0 & 0 & 0 \\ \widetilde{n}^T & 0 & 0 & 0 & -\widetilde{\mu} \\ \widetilde{D}^T & 0 & 0 & 0 & \widetilde{E} \\ 0 & 0 & \widetilde{\mu} & -\widetilde{E}^T & 0 \end{bmatrix} \begin{bmatrix} v \\ c_\nu \\ c_n \\ \widetilde{\beta} \\ \lambda \end{bmatrix} + \begin{bmatrix} -Mv^{(l)} - h_l k^{(l)} \\ 0 \\ \Gamma + \Delta \\ 0 \\ 0 \end{bmatrix} = \begin{bmatrix} 0 \\ 0 \\ \rho \\ \widetilde{\sigma} \\ \zeta \end{bmatrix} \tag{12}$$

$$\begin{bmatrix} c_n \\ \widetilde{\beta} \\ \lambda \end{bmatrix}^T \begin{bmatrix} \rho \\ \widetilde{\sigma} \\ \zeta \end{bmatrix} = 0, \qquad \begin{bmatrix} c_n \\ \widetilde{\beta} \\ \lambda \end{bmatrix} \geq 0, \qquad \begin{bmatrix} \rho \\ \widetilde{\sigma} \\ \zeta \end{bmatrix} \geq 0\,. \tag{13}$$

Here $\Gamma = \left(\Gamma^{(j_1)}, \Gamma^{(j_2)}, \ldots, \Gamma^{(j_s)}\right)^T$ is a nonnegative vector that has as many components as active constraints (elements in $\mathcal{A}$). It is clear that the solution of (12)–(13) coincides with the one of (6–7) if we can ensure that $\Gamma = \tilde{\mu}\Lambda$. To simplify the notation, we denote by $q^{(l)} = -Mv^{(l)} - h_l k^{(l)}$.

Important conclusions can be drawn from the observation that the mixed linear complementarity problem represents the optimality conditions of the quadratic program

$$\begin{array}{rll} \min_{v,\lambda} & \frac{1}{2} v^T M^{(l)} v + q^{(l)^T} v & \\ \text{subject to} & n^{(j)^T} v - \mu^{(j)} \lambda^{(j)} \geq -\Gamma^{(j)} - \Delta^{(j)}, & j \in \mathcal{A} \\ & D^{(j)^T} v + \lambda^{(j)} e^{(j)} \geq 0, & j \in \mathcal{A} \\ & \nu_i^T v = 0, & i = 1, 2, \ldots, p \\ & \lambda^{(j)} \geq 0 & j \in \mathcal{A}. \end{array} \tag{14}$$

In particular, since the quadratic program (14) is convex, it and therefore (12–13) can be solved in a time that is polynomial with the size of the problem. An issue is that the objective function of (14) is not strictly convex in λ that may lead to nonuniqueness of the solution, which is an obstacle in expressing sensitivity results with respect to the parameter Γ (which we will adjust iteratively so that the solution satisfies $\Gamma = \tilde{\mu}\Lambda$ and will thus be a solution of (6–7)). But this problem can be removed by noting that v, the velocity solution of (14) is a solution of the following quadratic program, that does not include λ:

$$\begin{aligned} \min_v \quad & \tfrac{1}{2} v^T M^{(l)} v + q^{(l)^T} v \\ \text{sbjct. to } & e^{(j)} n^{(j)^T} v + \mu^{(j)} D^{(j)^T} v \geq -\left(\Gamma^{(j)} + \Delta^{(j)}\right) e^{(j)}, \;\; j \in \mathcal{A} \\ & \nu_i^T v = 0, \;\; i = 1, 2, \ldots, p. \end{aligned} \tag{15}$$

Recall that we assume that $\Gamma^{(j)} \geq 0$ and $\Delta^{(j)} \geq 0$ for $j \in \mathcal{A}$. We note that this quadratic program is always feasible, because $v = 0$ is a feasible point. Moreover, it has a unique solution $v^*(\Gamma)$, since we assume that $M^{(l)}$ is positive definite. This allows us to define the mapping

$$P_1(\Gamma) = v^*(\Gamma). \tag{16}$$

Let v be a velocity vector. For the given active set $\mathcal{A}$, another useful function that we define is

$$\Lambda(v) = \lambda, \tag{17}$$

where

$$\lambda^{(j)} = \max_{i=1,2,\ldots,m_C^{(j)}} \left\{ d_i^{(j)^T}(v) \right\}, \quad j \in \mathcal{A}.$$

Because of the way $D^{(j)}$ is balanced for a given contact j, it can be shown that after $v^*(\Gamma)$, the solution of (15) is found, then a λ^*, that, together with $v^*(\Gamma)$, is a solution of (14) can be found by choosing

$$\lambda^* = \Lambda(v^*). \tag{18}$$

Therefore, all the properties of the velocity solution of (12–13) can be inferred by working with (15).

Our setup suggests the following iteration, after initializing with $\Gamma = 0$: Find a solution v^* of (15), compute $\Gamma = \tilde{\mu}\Lambda(v^*)$ and then proceed with the next iteration. We call this algorithm LCP1. We can see that the algorithm solves successively (15) which is a strictly convex quadratic program, which is why we call it a successive convex relaxation algorithm . The algorithm is in effect a fixed-point iteration for the mapping

$$\chi_1(v) = P_1(\tilde{\mu}\Lambda(v)). \tag{19}$$

The key to show that LCP1 ultimately converges to a fixed point, and thus, a velocity solution of (6–7) (since then we would have $P_1(\tilde{\mu}\Lambda(v^*)) = v^*$, and, by our previous observation concerning the relationship between (14) and (15), it follows that v^* is a solution of (6–7)) for sufficiently small friction is to show that it is a contraction, which is the following result.

Theorem 4.1

i *Consider the set* $S = \left\{ v \left| \|M^{(l)^{\frac{1}{2}}} v\|_2 \leq \|M^{(l)^{-\frac{1}{2}}} q^{(l)}\|_2 \right. \right\}$. *Then* $\chi_1(S) \subseteq S$.

ii *Assume that, for* $\tilde{\mu} = 0$, *the friction cone* $FC(q)$ *is pointed. Then there exists* $\mu^\circ > 0$ *such that whenever* $\|\tilde{\mu}\|_\infty \leq \mu^\circ$, *the mapping* $\chi_1(v)$ *is a contraction over* S *in the* $\|\cdot\|_\infty$ *norm, with parameter* $\frac{1}{2}$.

Sketch of the Proof The first part means that the kinetic energy at the end of the step cannot exceed the kinetic energy of the system with all constraints removed, and it follows much the same way as in [3]. The second part is based on the crucial observation that the friction cone is pointed if and only if MFCQ holds for the quadratic program (15). This allows us to apply the sensitivity results of [21] to conclude that $P_1(\Gamma)$ is a Lipschitz continuous mapping with parameter L (that does not depend on $\tilde{\mu}$ as soon as the friction cone is uniformly pointed, which is the critical technical difficulty) over S. The mapping $\Lambda(v^*)$ is uniformly Lipschitz with some parameter K_D which means that the mapping χ_1 is Lipschitz continuous with parameter $\|\tilde{\mu}\|_\infty LK_D$. The latter can be made smaller than $\frac{1}{2}$, provided that we choose $\|\tilde{\mu}\|_\infty$ to be sufficiently small, which completes the proof. For details, see [1]. ◇

As a part of the proof, we also have a lower bound on how small does the friction coefficient need to be in order to have our iterative algorithm converge. The key condition is $\|\tilde{\mu}\|LK_D < 1$, where L is the Lipschitz parameter of the mapping P_1 and K_D is the Lipschitz parameter of the mapping Λ. Therefore, a sufficient condition for the

convergence of our algorithm is

$$\tilde{\mu}^{(j)} \leq \frac{1}{LK_D},\ j \in \mathcal{A}.$$

The actual value of the Lipschitz parameters seems difficult to quantify in terms of significant dynamical characteristics.

An interesting conclusion occurs for our example in Section 3 that does have a pointed friction cone (in effect for any friction coefficient, following our duality interpretation, since it cannot get jammed, for any friction coefficient). At the same time, it has a nonconvex solution set for any nonzero friction coefficient. Based on the previous Theorem, our fixed-point iteration scheme based on successive convex relaxation will converge, for sufficiently small friction coefficients, with constant linear rate to the velocity solution of nonconvex problems while solving convex subproblems (that have polynomial complexity)!

For efficiency reasons, especially in real-time applications, one may wish to stop an iterative algorithm significantly before its convergence, perhaps even after one such step. In that case one may consider using as an approximation to the solution velocity just the first iteration of the fixed-point iteration for χ_1. The following result, which is based on the Lipschitz continuity properties of the solution of (15) estimates the error in velocity for this case.

Theorem 4.2 *Let $\mathcal{M}$ be a convex compact set such that $FC(q)$ is a pointed cone whenever $\hat{\mu} = \mathrm{diag}(\tilde{\mu}) \in \mathcal{M}$. Then there exists L, depending on $\mathcal{M}$ and S such that for any velocity solution v^* of (6–7) the following inequality holds:*

$$\|v^* - \chi_1(0)\|_\infty \leq L\|\tilde{\mu}\Lambda(v^*)\|_\infty.$$

Therefore $\chi_1(0)$, the solution of (15) when $\Gamma = 0$, approximates very well the solution of (6–7) when the product between the friction coefficient and the tangential velocity is small (though the friction coefficient itself does not need to be small). *In particular,* configurations that have a no slip solution are computed exactly by this method. We call LCP2 the time-stepping scheme that is based on one iteration of $\chi_1(0)$ (an thus one resolution of (15)). Comparing (12–13) with (6–7) we see that $\chi_1(0)$ satisfies all the constraints of (6–7) except the com-

plementarity constraint between the normal impulse and the normal velocity. This means that the velocity produced by LCP2 may predict take-off even when there is a nonzero normal impulse. The first part of Theorem 4.1 ensures that a time-stepping scheme based on $\chi_1(0)$ will in fact be stable since the inequality defining S is sufficient to generate a bounded velocity over any fixed time interval and for every timestep [3].

A. The logical flow of the algorithm

In this subsection we give a concise logical description of our algorithm.

1. Given $q^{(0)}$, $v^{(0)}$, $\tilde{\mu}$ (as a list of the possible friction coefficients), TOL > 0, $T > 0$, and $\epsilon > 0$, define $l = 0$ and $t^{(0)} = 0$.
2. Define the active set $\mathcal{A}$ as the set of $j \in \{1, 2, \ldots, p\}$ that satisfies $\Phi_c^{(j)}(q^{(l)}) \leq \epsilon$.
3. Compute $M(q^{(l)})$, $k(t^{(l)}, q^{(l)}, v^{(l)})$, $\tilde{D}(q^{(l)})$, $\tilde{\nu}(q^{(l)})$, $\tilde{n}(q^{(l)})$, h_l (that can be a constant time-step or a computed value from an adaptive algorithm), $\Delta(q^{(l)})$ and $q^{(l)} = -M(q^{(l)})v^{(l)} - h_l k^{(l)}$ from the user-supplied data, as defined after (6)–(7) and in Subsection A.
4. Define $k = 1$, $\Lambda(0) = 0$ and $\Gamma = \tilde{\mu}\Lambda(0)$.
5. Compute $v(k)$, the solution of (15).
6. Compute $\Lambda(k)$=$\Lambda(v(k))$, using (17) and define $\Gamma = \tilde{\mu}\Lambda(k)$.
7. If $\|\Lambda(k) - \Lambda(k-1)\| > TOL$ define $k = k + 1$ and go to 5.
8. Define $v^{(l+1)} = v(k)$.
9. Compute $q^{(l+1)} = q^{(l)} + h_l v^{(l+1)}$.
10. Ensure feasibility by a nonlinear projection on the set defined by (1) and (2) [2].
11. Define $t^{(l+1)} = t^{(l)} + h_{l+1}$.
12. If $t^{(l)} < T$ go to 3.

Table 1. Comparison between LCP0 and LCP2

μ	LCP0 CPU	LCP 2 CPU	LCP 2 Residual Error
0.1	29.76	34.42	0.06
0.2	MAX ITER	36.28	0.12
0.4	MAX ITER	24.03	0.07
0.6	MAX ITER	20.40	1e-8
0.8	MAX ITER	14.52	8e-11

B. Numerical Results

We have implemented the discussed algorithm in Matlab. We have simulated several two-dimensional cannonball arrangements with a variable number of disks of diameter 3: n disks placed on a long immovable plank, all in linear contact, then $n-1$ disks on top of these, and so forth. No joint constraints were considered.

The time step was chosen 0.05, constant throughout the simulation. All collisions are plastic and all simulations start with 0 velocity. This value of the time step corresponds to computing 20 frames per second and will result in output of sufficient quality for animation purposes. Of course, different applications may require smaller time-steps, as is the case for haptic interaction that requires time-steps no larger than 1 millisecond.

We denote by LCP0 Lemke's method applied to (6–7) (and which is guaranteed to find a solution [3]). To solve the linear complementarity problems (or the respective quadratic programs) we use PATH [11, 18].

We ran the following examples: (1) Arrangement with 21 disks, for friction $\mu = 0.05$ at all contacts. Four frames of the simulation are presented in Figure 2, with a three dimensional rendering. The stopping criteria for the iterative method LCP1 was $1e-5$ difference in $\Lambda(v)$ between iterations. The results are shown in Figure 3. (2) Arrangement with 136 disks and $\mu = 0.2$ for all contacts. Here LCP0 and LCP1 failed with a maximum number of iterations reached message (MAX ITER, $10,000$), so the results are plotted only for LCP2. The average normal velocity error (which we do not plot here) did

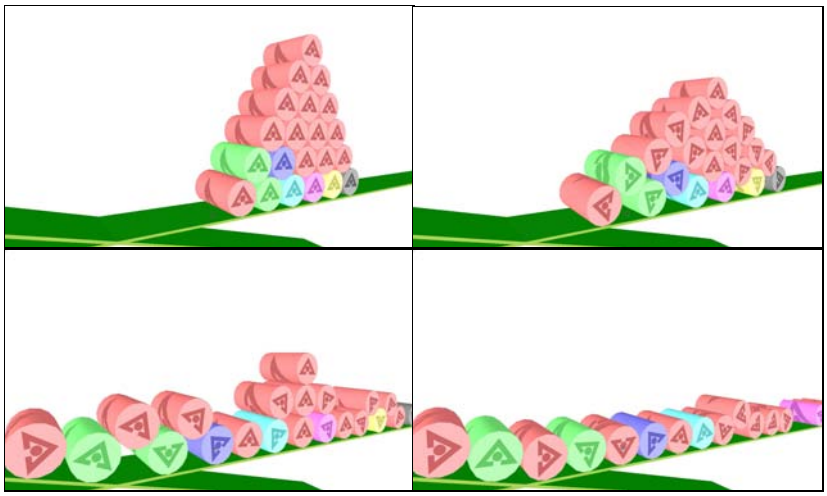

Figure 2. Four frames of a two-dimensional cannonball arrangement simulation involving 21 bodies

not exceed .12. (3) A comparison between LCP2 and LCP0 running times for 210 disks (20 on the bottom), for the first step of the simulation. The results are displayed in Table 1 for several values of the friction coefficients. The error is the error in normal velocity (for a contact (j) that satisfies $c_n^{(j)} > 0$, the normal velocity error is $\mu\lambda^{(j)}$) which is the only part violating the LCP constraints).

From the above mentioned figures and table we extract the following conclusions. (1) For a small number of bodies the Lemke solver solves LCP0 faster than our iterative method LCP1 but slower than LCP2. The situation for LCP1 can be considerably improved by applying specialized convex quadratic program solvers (a factor of 2 improvement will result from using Choleski instead of LU factorization as PATH currently does). Specialized techniques for convex QP approaches will be discussed in future research. (2) LCP1 has converged for 21 disks and $\mu = 0.05$, as predicted by the Theorem 4.1. (3) Other techniques (even if approximate) are essential for larger problems because, for 136 bodies, all solvers except LCP2 (the one iteration solver) failed on the problem. In such situations and given a

possible real-time constraint, users may have to accept approximate but fast solutions, like the ones provided by LCP2, which are at least valid in some fairly common cases. Note that for 21 bodies, both LCP0 and LCP2 solved the problem in substantially less than 50 ms most of the time, which would make the results compatible with real-time simulation. (4) We can also see that, in some cases, LCP1 and LCP2 do work faster than LCP0 (which actually fails on some of these problems), especially at high friction, near an equilibrium solution. This can be inferred from Table 1 (where LCP1 would stop at the last two cases if the stopping criteria was less than $1e-5$).

The results from table 1 seem to indicate that the larger the friction, the faster the results can be found by our iterative method. We believe that this an isolated occurence, that appears due to the fact that, since our cannonball configuration starts form 0 velocity, the larger the friction the closer the solution of (6–7) is to the 0 velocity solution for the next step (though the reaction impulses are not 0 at equilibrium). Since PATH [11, 18] is initialized with a 0 overall solution (both velocity and impulses), it is closer in the solution space to the final solution for larger friction coefficients.

5. Conclusions

We construct an algorithm for the linear complementarity problem that appears in certain time-stepping schemes [22, 3]. We show that even simple problems such as the example presented in Section 3 may have a nonconvex solution set at 0 velocity, for arbitrarily small but nonzero friction.

We show that for sufficiently small friction a fixed-point iteration (successive convex relaxation) approach converges linearly to the intended velocity solution provided that the friction cone is pointed. Fixed-point iterations have been used in the past to solve friction problems for small friction coefficients [8, 19, 20]. Nevertheless, our method is different from previous approaches in that we obtain convergence even for configurations for which the impulse or force part of the solution is not unique, or the solution set may not even be

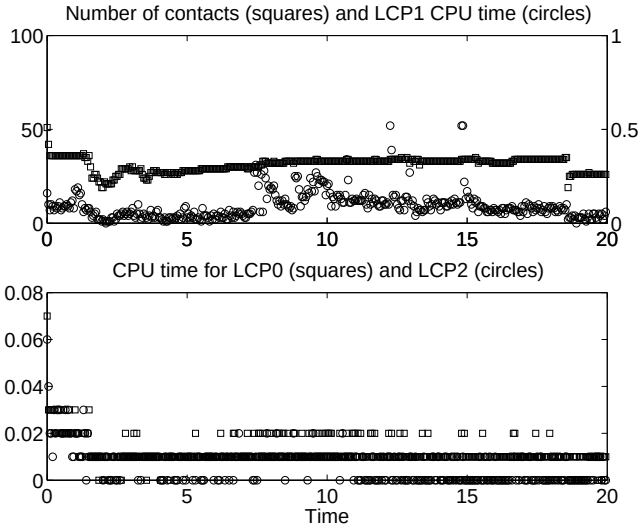

Figure 3. Comparison of a 2D simulation with 21 bodies

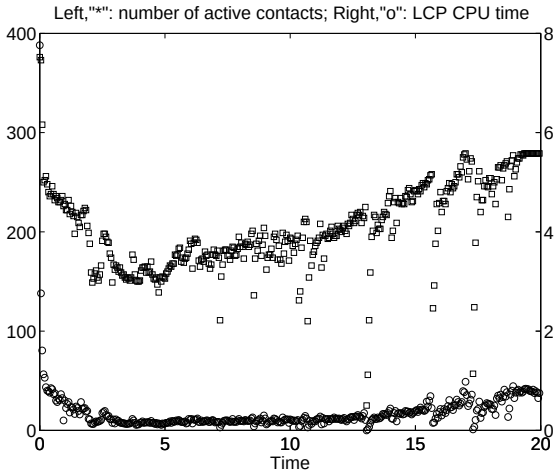

Figure 4. Results of a 2D simulation with 136 bodies

convex (though the velocity may be unique).

It is true that, at small friction, the classical acceleration-force model may have a solution and the development that treats the problem in impulse–velocity coordinates may not be necessary to get a consistent framework [14]. If the friction is treated implicitly, however, then one would have to solve at every step the linear complementarity problem (6–7) [2]. The implicit treatment of friction (in the sense that dissipation is enforced based on the velocity at the end of the interval) is useful because of the good energy properties [2, 3]. Therefore, the approach (6–7) is relevant even when the configuration is consistent in a classical sense but the discrete scheme needs to preserve the energy properties of the continuous model. Such a situation occurs when one needs to run the simulation for a long period of time, which is the case in many interactive simulations, where the drift in energy could become significant over a long period of time, especially if it is increasing.

We also demonstrate that efficient approximations of the linear complementarity problem (6–7) can be constructed by using only one linear complementarity problem (or, equivalently, one convex quadratic program) per step. This approximation has very low error when the product between the friction coefficient and the tangential velocity at the contact is small, can solve efficiently configurations with hundreds of bodies, and results in a time-stepping scheme with good energy properties of the simulation. Such approximations may prove useful for real-time simulations where the users may be unwilling to let costly algorithms run to completion and where a coarse approximation that is physically meaningful may be sufficient.

Acknowledgments

Thanks to Todd Munson and Mike Ferris for providing and supporting PATH [11, 18].

References

1. Anitescu, M., and Hart, Gary D. "A Fixed-Point Iteration Approach for Multibody Dynamics with Contact and Small Friction", Preprint ANL/MCS-P985-0802, Mathematics and Computer Science Division, Argonne National Laboratory, 2001.
2. Anitescu, M., and Potra, F. A., "A time-stepping method for stiff multibody dynamics with contact and friction", *International Journal for Numerical Methods in Engineering*, **55**: 753–784, 2002.
3. Anitescu, M., and Potra, F. A., "Formulating rigid multi-body-dynamics with contact and friction as solvable linear complementarity problems", *Nonlinear Dynamics* **14**, 231–247, 1997.
4. Anitescu, M., Stewart, D. and Potra,F. A., "Time-stepping for three-dimensional rigid body dynamics", *Computer Methods in Applied Mechanics and Engineering* **177**(3–4), 183–197, 1999.
5. Anitescu, M., Lesaja, G., and Potra, F. A. Equivalence between different formulations of the linear complementarity problems, *Optimization Methods and Software* **7** (3-4), 265-290, 1997.
6. Anitescu, M., Cremer, J., and Potra, F. A., "Formulating 3D contact dynamics problems", *Mechanics of Structures and Machines* **24**(4), 405-437, 1996.
7. Anitescu, M., Cremer,J. F. and Potra, F. A. "Properties of complementarity formulations for contact problems with friction" in *Complementarity and Variational Problems: State of the Art*, edited by Michael C. Ferris and Jong-Shi Pang, SIAM Publications, Philadelphia, 1997, pp. 12-21.
8. Bisegna, P., Lebon, F. and Maceri, F. "D-PANA: A convergent block-relaxation solution method for the discretized dual formulation of the Signorini-Coulomb contact problem" *Comptes rendus de l'Academie des sciences - Serie I - Mathematique* **333**(11), 1053-1058, 2001.
9. Cottle, R. W., Pang, J.-S, and Stone, R. E., *The Linear Complementarity Problem*, Academic Press, Boston, 1992.
10. Cremer, J., and Vanecek G., "Building simulations for virtual environments", *Proceedings of the IFIP International Workshop*

on Virtual Environments, October 1994, Coimbra, Portugal.
11. Dirkse, S. P., and Ferris, M. C., "The PATH solver: A non-monotone stabilization scheme for mixed complementarity problems", *Optimization Methods and Software* **5**, 123–156, 1995.
12. Glocker, Ch. and Pfeiffer, F., 'Multiple impacts with friction in rigid multi-body systems', *Nonlinear Dynamics* **7**, 1995, 471-497.
13. Pfeiffer, F. and Glocker, Ch, *Multibody dynamics with unilateral contacts*, John Wiley & Sons Inc., New York, 1996,
14. Lo, G., Sudarsky, S., Pang, J.-S. and Trinkle, J. "On dynamic multi-rigid-body contact problems with Coulomb friction," *Zeitschrift fur Angewandte Mathematik und Mechanik* **77**, 267–279, 1997.
15. Haug, E. J., *Computer Aided Kinematics and Dynamics of Mechanical Systems*, Allyn and Bacon, Boston, 1989.
16. Mangasarian, O. L., *Nonlinear Programming*, McGraw-Hill, New York 1969.
17. Mangasarian, O. L. and Fromovitz, S., "The Fritz John necessary optimality conditions in the presence of equality constraints", Journal of Mathematical Analysis and Applications 17 (1967), pp. 34-47.
18. Munson, T. S., "Algorithms and Environments for Complementarity", Ph.D. thesis, Department of Computer Science, University of Wisconsin-Madison, 2000.
19. Necas, J., Jarusek, J. and Haslinger, J,: "On the solution of the variational inequality to the Signorini problem with small friction", *Bulletino U.M.I.* **17B**, 796–811, 1980.
20. Panagiotopoulos, P. D., *Hemivariational Inequalities*. Springer-Verlag, New York, 1993.
21. Robinson, S.M., "Generalized equations and their solutions, part II: Applications to nonlinear programming", *Mathematical Progamming Study* **19**, 200–221, 1982.
22. Stewart, D. E., and Trinkle, J. C., "An implicit time-stepping scheme for rigid-body dynamics with inelastic collisions and Coulomb friction", *International J. Numerical Methods in Engineering* **39**, 2673-2691, 1996.
23. Stewart, D., "Rigid-body dynamics with friction and impact",

SIAM Review **42** (1), 3–29, 2000.